Kollar, László E., Farzaneh, Masoud and Van Dyke, P.

Modeling of cable vibration following ice shedding propagation

## Original Citation

Kollar, László E., Farzaneh, Masoud and Van Dyke, P. (2011) Modeling of cable vibration following ice shedding propagation. In: IWAIS 2011 - The 14th International Workshop on Atmospheric Icing of Structures, 8-13th May 2011, Chongqing, China. (Unpublished)

# Modeling of Cable Vibration Following Ice Shedding Propagation

László E. Kollár, Masoud Farzaneh
*NSERC/Hydro-Québec/UQAC Industrial Chair on Atmospheric Icing of Power Network Equipment (CIGELE) and Canada Research Chair on Atmospheric Icing Engineering of Power Networks (INGIVRE)* www.cigele.ca
Université du Québec à Chicoutimi (UQAC)
Chicoutimi, Qc, Canada
*E-mail:* laszlo_kollar@uqac.ca

Pierre Van Dyke
*Hydro-Québec Research Institute – IREQ*
Hydro-Québec
Varennes, Qc, Canada

***Abstract*—The dynamic effects induced by ice shedding propagation on overhead transmission line cables are simulated numerically. The numerical model is validated by comparing simulation results to observations made on the full-scale test line of Hydro-Québec. The uniform ice load is simulated by several concentrated loads acting at constant distances along the loaded span. Ice shedding propagation is then simulated through the removal in a defined sequence of the concentrated loads. The model thus built can predict some parameters describing the dynamic behavior of the span during the vibration following the ice shedding propagation, such as the time history of cable tension and displacement as well as the period of vibration. The decay of vibration may also be forecasted once the cable damping is properly defined in the model. The numerically obtained results show close agreement with the experimental observations, which fact confirms the reliability of the model and its applicability for predicting the dynamic effects of ice shedding propagation on an overhead line conductor.**

***Keywords-cable vibration; full-scale experiment; ice shedding; numerical modeling; overhead transmission line***

## I. INTRODUCTION

Shedding of large ice chunks from transmission line cables leads to high-amplitude vibration and excessive transient dynamic forces. High conductor rebound may trigger flashovers whereas the dynamic loads may cause suspension failure and even cascading damage to several towers. These problems justify the particular interest in cold climate regions to predict the cable jump height as well as the tension developing in the cable and at the suspension during cable vibration following ice shedding. This information allows us to evaluate the severity of the phenomenon.

Field observation of ice shedding is a difficult task, because of the unforeseeable and non-repetitive occurrence of the phenomenon. Therefore, great effort has been made to simulate ice shedding numerically and experimentally on small-scale or full-scale test lines. Numerical models have been developed using a commercial finite element software ADINA [1]. These models were applied to simulate ice shedding from a single conductor [2, 3] or from conductor bundles [4, 5]. Small-scale experimental setups were constructed in order to validate the numerical models [2]. Ice shedding on full-scale test lines was simulated by load dropping tests [6]. All of these models considered sudden ice shedding from one conductor or from a part of one conductor when modeling partial shedding. However, ice shedding propagation along the span is a more representative process of the natural shedding phenomenon than sudden shedding. More recently, full-scale experiments were designed to simulate ice shedding propagation along a span of the Hydro-Québec test line [7]. The main objectives of the present study is to develop a numerical model which is applicable to simulate ice shedding propagation, and to validate the model by comparing the results to observations made on the full-scale test line in [7].

## II. NUMERICAL MODEL

The numerical model for simulating ice shedding propagation from one span on a transmission line is presented in this section. This model is implemented using the finite element analysis software ADINA [1]. The model of the transmission line elements including cable and suspension strings is based on former publications [2, 3]. The cable damping is considered following the recommendation of [8]. The model of ice shedding propagation is developed in the present paper.

### A. *Transmission Line Elements*

The cable is modeled by two-node isoparametric truss elements with large kinematics. A constant initial pre-strain corresponding to the installation conditions is prescribed as an initial condition for all cable elements. The material properties of the cable are accounted for by a nonlinear elastic material model, not allowing compression and assuming Hookian small-strain behaviour in tension [2, 3]. The cable is assumed to be perfectly flexible in bending and torsion. The mesh contains 100 cable elements in each span.

The cable damping is considered as Rayleigh damping as proposed in [8]. In this case the damping matrix is a linear combination of the mass matrix and stiffness matrix, and the Rayleigh damping coefficients are obtained from the natural circular frequencies and damping ratios, respectively, in two different vibration modes [9].

The suspension strings are modelled by beam elements and by elastic isotropic material properties with constant cross-section. They are allowed to swing freely in the vertical plane during cable vibration [2, 3].

### B. *Ice Load and Shedding Propagation*

Although ice load usually appears on conductors as a distributed load, this model will consider ice load by several concentrated loads acting at constant distances along the loaded span. Modeling ice load this way makes the simulation of shedding propagation possible by removing any of the concentrated loads at arbitrary time instants. Furthermore, it facilitates the simulation of the full-scale tests [7] where the load was also attached at several discrete points along a span. Ice shedding propagation is then simulated through the removal in a defined sequence of the concentrated loads. The propagation velocity is controlled by associating each concentrated load with a time function which determines the removal time of that specific load.

The characteristics of time function which defines a load removal is shown in Fig. 1(a). The time, $t_i$, denotes the beginning of load removal, $\Delta t_r$ stands for time interval of load removal, and $\Delta t_s$ is the time step in the numerical simulation. It is assumed that a load is removed suddenly, i.e. $\Delta t_r < \Delta t_s$. This time function is applied for each load at different time instances. If $n$ loads act along the span and $T_w$ denotes the wave propagation time along the span, then the time instance when the defined time function is applied for the $i$th load may be determined as follows:

$$t_i = \frac{i}{n+1} T_w \qquad\qquad i = 1,\ldots,n$$

An alternate time function is also applied in the model, because the previous time function does not consider an important effect that occurs when the ice chunk shed from a part of the conductor does not break off the ice which is still attached to the remaining part of the conductor. When ice sheds, the cable is unloaded at that position. However, the falling ice applies an excess load on the conductor where the ice is still attached. The tests presented in [7] simulate such processes. Thus, numerical modeling will also be carried out by applying the time function shown in Fig. 1(b). The models using the time functions shown in Figs. 1(a) and 1(b) will be called Model-1 and Model-2, respectively.

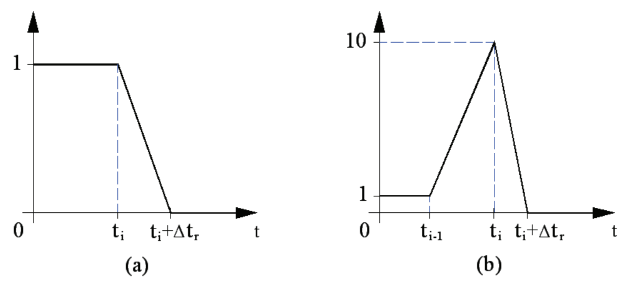


Figure 1. Time functions for load removal

## III. Application for Ice Shedding Propagation from a Full-Scale Test Line

### A. *Numerical Model of Hydro-Québec Test Line*

The Hydro-Québec test line consists of three suspension spans and two dead-end spans. Ice shedding propagation on the middle span from a single conductor and from vertical arrangements of three conductors was simulated in [7]. Ice weight was modeled by a conductor which was held initially by pulleys at each end of the span, and which was connected to the test conductor by strings at every 15 m along the span. The load simulated this way was 0.6 kg/m. Shedding was initiated by releasing the pulley at one end of the span, and then the strings broke one after the other simulating the propagation of load shedding. It took 3 s to break all the strings holding the dead-weight conductor in the tests with a single conductor. Geometrical data on the line are provided in Fig. 2 which is a sketch of the numerical model of the unloaded test line. The ice shedding tests were performed on Condor conductors suspended with I-insulator strings. Geometrical and material data of the conductor and insulator strings are shown in Table I. The conductor damping is due mainly to aerodynamic resistance whereas structural damping is several orders of magnitude smaller [10]. The damping coefficient due to aerodynamic resistance in the first vibration mode was determined as 0.01 in [10], and the Rayleigh damping coefficients were obtained in this case using the natural circular frequencies and damping ratios in the first symmetric and antisymmetric modes.

The numerical model considered all the five spans as shown in Fig. 2. The dead-end spans were fixed to the ground allowing no displacement and no rotation of the endpoints. The towers were assumed to be rigid, i.e. no displacement was allowed at the fixed ends of suspensions, but the suspensions were allowed to rotate around the suspension point in the vertical plane of the set-up. The sag of the middle span without load was determined in correspondence with the original set-up [7]. The profiles of the other four spans were obtained from the condition that the cable tension in the unloaded set-up should be the same in all the spans. The load was modeled by concentrated loads at every 15 m, thereby applying 29 loads along the 450-m-long middle span. As the length of a cable element was chosen to be 3 m there were 5 cable elements between two loads. Load removal was controlled by time functions described in Section II.B so that the whole span is unloaded in 3 s. Thus, $T_w = 3$ s, $n = 29$, and the time between the

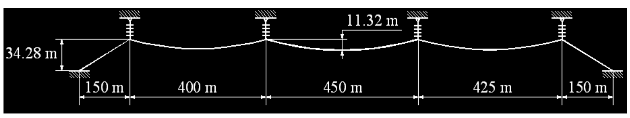


Figure 2. Sketch of numerical model of the unloaded test line (vertical dimensions are exaggerated)

TABLE I. GEOMETRICAL AND MATERIAL DATA OF CONDUCTOR AND INSULATOR

| Parameter | Unit | Value |
|---|---|---|
| Conductor type | – | Condor ACSR 54/7 |
| Conductor diameter | (mm) | 27.8 |
| Cross-sectional area of the conductor | ( $mm^2$ ) | 455.1 |
| Mass per unit length of the conductor | (kg/m) | 1.522 |
| Conductor density | ( $kg/m^3$ ) | 3337 |
| Young's modulus of the conductor | (GPa) | 68.3 |
| Insulator length | (m) | 1.8 |
| Insulator mass | (kg) | 8.2 |
| Insulator density | ( $kg/m^3$ ) | 2700 |
| Young's modulus of the insulator | (GPa) | 70 |
| Poisson's ratio | – | 0.3 |

removal of two consecutive loads is 0.1 s. The time step of the computation was chosen to be $\Delta t_s$ = 0.01 s and $\Delta t_s$ = 0.005 s in Model-1 and in Model-2, respectively.

### *B. Results*

The load was applied on the cable in the static analysis. The resulting profile is shown in Fig. 3. There is an excellent agreement between the calculated and measured additional displacements at mid-span. The sag of the unloaded cable was 11.32 m, which increased by 2.8 m in the experiments and by 2.76 m according to the numerical model. On the other hand, there is a discrepancy between calculated and measured results at positions closer to Tower 3. Greater displacement was measured at 150 m than at mid-span which may be due to the asymmetry of the configuration (different lengths of the neighboring spans), although the effect of this asymmetry is less significant according to the numerical simulation. The cable tension in the unloaded span was 33.4 kN, which increased to 36.6 kN in the experiment and to 37.7 kN in the numerical modeling.

The dynamic analysis provided the time histories of cable displacement and cable tension. Fig. 4 presents the cable jump at different positions along the span, i.e. the maximum vertical displacement above the loaded position. Model-1 underestimates this jump. However, when the alternate time function is applied, the model provides a close prediction of the experimental results.

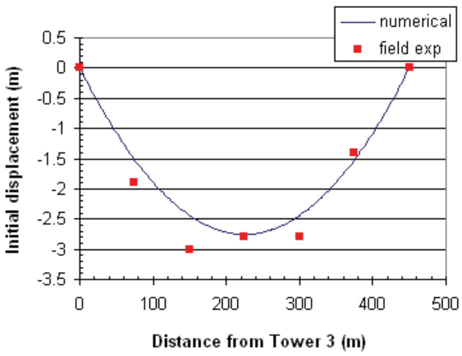


Figure 3. Cable deformation in the loaded static equilibrium

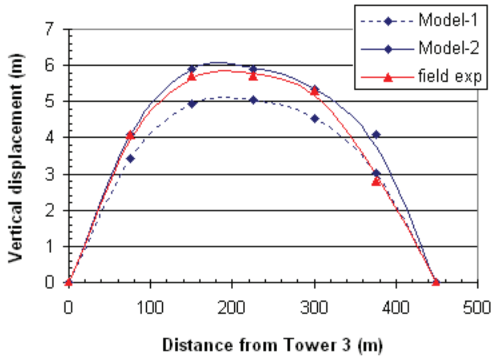


Figure 4. Cable jump during ice shedding propagation

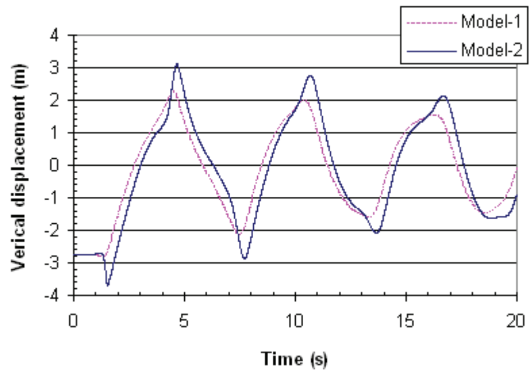


Figure 5. Time history of cable displacement at mid-span as obtained numerically

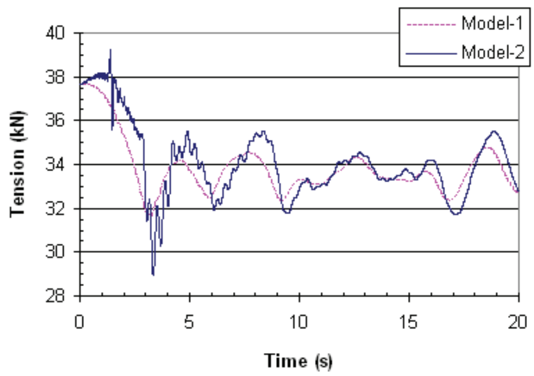


Figure 6. Time history of cable tension at mid-span as obtained numerically

The time histories of cable displacement and cable tension at mid-span are drawn in Figs. 5 and 6, respectively. The whole span sheds in 3 s, so that the shedding propagation arrives to mid-span after 1.5 s. The cable at mid-span does not move noticeably in the first 1.5 s of the simulation. At the same time, the cable tension decreases slightly when using Model-1 and increases slightly according to Model-2. The vibration amplitude is greater in the latter case due to the abrupt increase of the load preceding shedding. A small drop in the cable position and a small peak in the cable tension when ice sheds at mid-span

TABLE II. COMPARISON OF NUMERICALLY AND EXPERIMENTALLY OBTAINED CABLE DISPLACEMENT AND TENSION AT MID-SPAN; (D) – DISPLACEMENT TIME HISTORY, (T) – TENSION TIME HISTORY

| Parameter | Unit | Num. Model-1 | Num. Model-2 | Field Exp. [7] |
|---|---|---|---|---|
| Period (D) | (s) | 5.73 | 5.77 | 5.8 |
| Frequency (D) | (Hz) | 0.175 | 0.173 | 0.17 |
| Drop (D) | (m) | -0.03 | -0.97 | -1.4 |
| 1st ampl. (D) | (m) | 5.07 | 6.83 | 7.15 |
| Jump (T) | (kN) | 0.0018 | 1.57 | 2.5 |
| 1st ampl. (T) | (kN) | 6.09 | 10.33 | 9.8 |

(1.5 s after the shedding propagation begins) may also be observed in the latter case similarly to what was reported in [7].

Some characteristics of the computed and measured time histories are compared in Table II. The period, and consequently the frequency, of vibration in the numerical simulation and in the experimental tests coincide. The initial drop in the cable position and the initial peak in the cable tension are almost non-existent in the simulation by Model-1, and they are underestimated even by Model-2. However; the first amplitude, i.e. the difference between the first maximum and minimum, in both time histories are predicted with an error of less than 5% by Model-2, and they are significantly underestimated by Model-1. Thus, Model-2 provides a close approximation of the propagating shedding phenomenon simulated experimentally on a full-scale test line in [7]. However, if the ice sheds in chunks which break off the remaining part of the ice then Model-1 will probably be a better choice for simulation.

## IV. CONCLUSION

A numerical model has been developed for simulating the propagation of ice shedding on transmission line cables. The ice load was simulated by several concentrated loads applied along the span, and the shedding propagation by their consecutive removal. The load removal was controlled by a time function which could be adjusted according to the modeled phenomenon. The model was applied for an experimental simulation carried out on a full-scale test line in a previous study. The model was validated by comparing the numerical results to the following measured parameters: cable profile and tension in the static equilibrium of the loaded span, maximum cable displacement above the loaded position during the vibration following propagating shedding, and time histories of cable displacement and tension during the same vibration. The close agreement of numerical and experimental results suggests that the model is a reliable tool to simulate ice shedding propagation.


## ACKNOWLEDGMENT

This work was carried out within the framework of the NSERC/Hydro-Quebec/UQAC Industrial Chair on Atmospheric Icing of Power Network Equipment (CIGELE) and the Canada Research Chair on Engineering of Power Network Atmospheric Icing (INGIVRE) at Université du Québec à Chicoutimi. The authors would like to thank the CIGELE partners (Hydro-Québec, Hydro One, Réseau Transport d'Électricité (RTE) and Électricité de France (EDF), Alcan Cable, K-Line Insulators, Tyco Electronics, Dual-ADE, and FUQAC) whose financial support made this research possible.


## REFERENCES


[1] ADINA, "Theory and Modeling Guide", Watertown, MA, 2004.

[2] A. Jamaleddine, G. McClure, J. Rousselet, and R. Beauchemin, "Simulation of Ice Shedding on Electrical Transmission Lines Using ADINA," *Computers & Structures,* vol. 47, no. 4/5, pp. 523-536, 1993.

[3] M. Roshan Fekr, and G. McClure, "Numerical modelling of the dynamic response of ice shedding on electrical transmission lines," *Atmospheric Research,* vol. 46, pp. 1-11, 1998.

[4] L. E. Kollár, and M. Farzaneh, "Dynamic behavior of cable systems with spacers following ice shedding," in *Proc. ICNPAA: Mathematical Problems in Engineering and Aerospace Sciences*, Budapest, Hungary, 2006, pp. 399-406.

[5] L. E. Kollár, and M. Farzaneh, "Vibration of Bundled Conductors Following Ice Shedding," *IEEE Trans. on Power Delivery,* vol. 23, no. 2, pp. 1097-1104, 2008.

[6] V. T. Morgan, and D. A. Swift, "Jump height of overhead-line conductors after the sudden release of ice loads," *Proceedings of IEE,* vol. 111, no. 10, pp. 1736-1746, 1964.

[7] P. Van Dyke, and A. Laneville, "Simulated Ice Shedding on a Full-Scale Test Line," in *Proc. 8th Int. Symp. on Cable Dynamics*, Paris, France, 2009.

[8] M. Roberge, "A Study of Wet Snow Shedding from an Overhead Cable," Department of Civil Engineering and Applied Mechanics, McGill University, Montreal, QC, 2006.

[9] K.-J. Bathe, *Finite Element Procedures*, Upper Saddle River, NJ: Prentice-Hall, 1996.

[10] P. Van Dyke, "Galop induit sur une ligne expérimentale à l'aide de profilés en D sur conducteur simple avec ou sans entretoises interphases," Ph.D. thesis, Department of Mechanical Engineering, University of Sherbrooke, Sherbrooke, QC, 2007.